Oncogene (2006) 25, 6262–6276

www.nature.com/onc

ORIGINAL ARTICLE

Functional analysis of the regulatory requirements of B-Raf and the B-Raf^{V600E} oncoprotein

T Brummer[1,2], P Martin[2], S Herzog[2], Y Misawa[2,3], RJ Daly[1] and M Reth[2]

[1]*Cancer Research Program, The Garvan Institute of Medical Research, Sydney, NSW, Australia;* [2]*Department of Molecular Immunology, Institute for Biology III, Albert-Ludwigs-University of Freiburg and Max-Planck-Institut for Immunobiology, Freiburg, Germany and* [3]*Department of Microbiology, University of Virginia Health System, University of Virginia, Charlottesville, VA, USA*

The *BRAF^{V600E}* mutation is found in approximately 6% of human cancers and mimics the phosphorylation of the kinase domain activation segment. In wild-type B-Raf (B-Raf^{wt}), activation segment phosphorylation is thought to cooperate with negative charges within the N-region for full activation. In contrast to Raf-1, the N-region of B-Raf is constitutively negatively charged owing to the presence of residues D447/D448 and the phosphorylation of S446. Therefore, it has been suggested that this hallmark predisposes B-Raf for oncogenic activation. In this study, we demonstrate that neutralizing mutations of these residues (in particular S446 and S447), or uncoupling of B-Raf from Ras-guanine 5′-triphosphate (GTP), strongly reduce the biological activity of B-Raf in a PC12 cell differentiation assay. We also confirm that S365 is a 14-3-3 binding site, and determine that mutation of this residue rescues the impaired biological activity of B-Raf proteins with a neutralized N-region, suggesting that the N-region opposes a 14-3-3-mediated transition into an inactive conformation. However, in the case of B-Raf^{V600E}, although complete N-region neutralization resulted in a 2.5-fold reduction in kinase activity *in vitro*, this oncoprotein strongly induced PC12 differentiation or transformation and epithelial–mesenchymal transition of MCF-10A cells regardless of its N-region charge. Furthermore, the biological activity of B-Raf^{V600E} was independent of its ability to bind Ras-GTP. Our analysis identifies important regulatory differences between B-Raf^{wt} and B-Raf^{V600E} and suggests that B-Raf^{V600E} cannot be inhibited by strategies aimed at blocking S446 phosphorylation or Ras activation.
Oncogene (2006) **25,** 6262–6276. doi:10.1038/sj.onc.1209640; published online 15 May 2006

Keywords: Ras; 14-3-3 proteins; β-Catenin; E-cadherin; mammary epithelial cells

Correspondence: Dr T Brummer, Cancer Research Program, The Garvan Institute of Medical Research, 384 Victoria Street, Sydney, NSW 2010, Australia.
E-mail: t.brummer@garvan.org.au
Received 16 September 2005; revised 20 March 2006; accepted 21 March 2006; published online 15 May 2006

Introduction

The Ras/Raf/mitogen-activated/extracellular-regulated kinase (MEK)/extracellular signal regulated kinase (ERK) pathway plays a pivotal role in control of proliferation and differentiation and, owing to its role as a gatekeeper of this pathway, Raf appears an attractive therapeutic target (O'Neill and Kolch, 2004; Wilhelm *et al*., 2004). The Raf-kinase family comprises the A-Raf, B-Raf and Raf-1 isoforms in vertebrates as well as D-Raf and LIN-45 in *Drosophila* and *Caenorhabditis*, respectively. B-Raf, the major ERK activator in vertebrates, is required for the maintenance of basal ERK activity and displays the most potent transforming activity (Papin *et al*., 1998; Brummer *et al*., 2002; Mercer and Pritchard, 2003). All isoforms share three highly conserved regions (CRs; Figure 1a): the N-terminal CR1 contains the Ras-guanine 5′-triphosphate (GTP)-binding domain (RBD), which initiates the interaction with Ras-GTP through a conserved arginine residue (R188 in B-Raf) that is required for the recruitment and activation of Raf at the plasma membrane. Consequently, mutation of this residue prevents Ras/Raf interaction and renders D-Raf, B-Raf and Raf-1 unresponsive to most extracellular signals (Hou *et al*., 1995; Marais *et al*., 1997; Brummer *et al*., 2002). The CR2 contains a negative regulatory serine residue (S259 and S365 in Raf-1 and B-Raf, respectively) that is proposed to serve as a binding site for 14-3-3 proteins, although this has only been confirmed for Raf-1 (Roy *et al*., 1998; Hekman *et al*., 2004). The catalytic domain (CR3) harbours phosphorylation sites for Raf-regulating enzymes within two segments, the N-region and the activation segment (Mercer and Pritchard, 2003). All isoforms carry a second 14-3-3 binding motif at the C-terminal end of the CR3 domain and its mutation abrogates the biological activity of B-Raf, Raf-1 and LIN-45, demonstrating also a conserved positive role of 14-3-3 proteins for the coupling of Raf to downstream effectors (MacNicol *et al*., 2000; Light *et al*., 2002; Harding *et al*., 2003).

So far, most studies have focused on the activation of Raf-1 and the following model of Raf-1 activation has emerged: In unstimulated cells, Raf-1 is phosphorylated on S259 and S621 (S365 and S729 in B-Raf), which mediate its binding to a 14-3-3 protein dimer (Roy *et al*.,

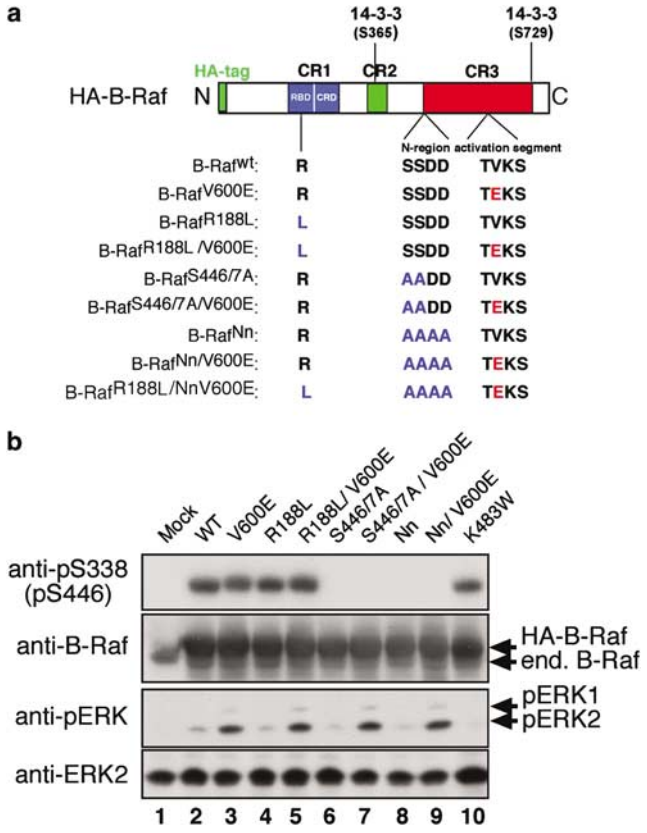

Figure 1 The V600E mutation confers a high signalling potential to B-Raf regardless of its N-region charge or ability to interact with Ras-guanine 5′-triphosphate (GTP). (**a**) Domain structure of hemagglutinine (HA)-tagged B-Raf (HA-B-Raf) proteins and location of the Ras/B-Raf interaction-regulating amino-acid residue R188, the N-region (S446/S447/D448/D449-sequence (SSDD-sequence)) and the activation segment (TVKS-sequence) and their corresponding mutants. Inhibiting and activating mutations are shown in blue and red, respectively. The two 14-3-3 binding motifs are also indicated. (**b**) Activation of extracellular signal regulated kinase (ERK) by B-Raf and its mutants. HEK293/EBNA-2 cells were transfected with the indicated constructs. After 48 h, N-region phosphorylation was monitored using an antibody recognizing phosphorylated S446 (pS446). Hemagglutinine (HA)-tagged B-Raf and endogenous B-Raf were detected with an anti-B-Raf antibody. Active ERK-1,2 molecules were detected using an anti-phospho-ERK antibody. A representative experiment is shown.

1998; Hekman *et al*., 2004). This dimer is proposed to tether the regulatory and catalytic lobes together and thereby stabilize a closed, inactive conformation of Raf-1. Upon binding to Ras-GTP, 14-3-3 is displaced from phospho-S259 and its re-binding is prevented by S259 dephosphorylation (Dhillon *et al*., 2002). This induces an open conformation leading to the exposure of the MEK docking site and the phosphorylation of the N-region and activation segment (Chong *et al*., 2001; Terai and Matsuda, 2005). The N-region plays a critical role in Raf activation (Mason *et al*., 1999). Negative charges within this region are required for activation and enhance the affinity of Raf-1 towards its substrate MEK (Xiang *et al*., 2002). Raf-1 activation involves an inducible two-step mechanism leading to Ras-dependent phosphorylation of the N-region residues S338/339 and Y340/341 at the plasma membrane (Mason *et al*., 1999; Carey *et al*., 2003). In contrast, the N-region of B-Raf is permanently negatively charged owing to the presence of the D448/449, which occupy positions equivalent to Y340/341 in Raf-1, and the constitutive phosphorylation of the S338 equivalent (S446) (Mason *et al*., 1999; Brummer *et al*., 2002). The charged N-region of B-Raf is, at least in part, responsible for its high basal *in vitro* kinase activity, as mutation of the S446/S447/D448/D449 sequence (referred to as SSDD sequence in the following) results in drastic reduction of both basal and Ras-GTP-stimulated *in vitro* kinase activities (Marais *et al*., 1997; Mason *et al*., 1999). The importance of the SSDD sequence is partially explained by the crystal structure of the isolated B-Raf kinase domain in which D^{448} was shown to stabilize the active conformation through a salt-bridge with R^{506} of the αC-helix (Garnett and Marais, 2004; Wan *et al*., 2004). These observations have led to a model in which the constitutive N-region charge primes B-Raf for full activation by Ras-GTP-triggered activation segment phosphorylation at the membrane (Brummer *et al*., 2002; Garnett and Marais, 2004; Morrison, 2004). However, as the aforementioned crystal structure is based on a dephosphorylated protein, the importance of the serine residues within the N-region is less understood. In striking contrast to Raf-1 S338 phosphorylation, phosphorylation of the evolutionary conserved S446 in B-Raf is neither stimulated by nor dependent on Ras-GTP/B-Raf interaction (Mason *et al*., 1999; Brummer *et al*., 2002) and is not affected by lipid raft disruption (Carey *et al*., 2003). This suggests not only that S446 phosphorylation occurs prior to interaction with Ras-GTP but also that Raf-1 and B-Raf are phosphorylated in different subcellular locations and/or by distinct N-region kinases. Hence, these findings raise the possibility that the currently unidentified S446 kinase represents an isoform-specific Achilles heel for the inhibition of B-Raf. However, the importance of the N-region has not been addressed for full-length B-Raf in a biological system.

Another critical event in Raf activation is the Ras-GTP-triggered phosphorylation of the activation segment (T599 and S602 in human B-Raf; Zhang and Guan, 2000). As N-region and activation segment phosphorylation act synergistically in Raf-1 activation (Chong *et al*., 2001), it has been suggested that the constitutively charged N-region predisposes B-Raf for oncogenic hits (Davies *et al*., 2002; Morrison, 2004; Wellbrock *et al*., 2004a). Indeed, gain-of-function mutations in the human *BRAF* gene have been identified in about 70% of malignant melanomas, 30% of papillary thyroid and serous ovarian carcinomas, 15% of colorectal cancers and to a lower frequency in a wide range of other tumours (Davies *et al*., 2002; Garnett and Marais, 2004). The majority of these mutations (91%) lead to substitution of valine 600 by glutamic acid ($B\text{-}Raf^{V600E}$) mimicking the conformational change of the activation segment induced by T599 and S602 phosphorylation (Garnett and Marais, 2004; Wan *et al*., 2004). Tumours carrying a $BRAF^{V600E}$ allele

display high MEK/ERK activity and the growth of their xenografts is highly dependent on this pathway (Solit *et al*., 2006). Expression of B-Raf^{V600E} has been shown to transform fibroblasts and melanocytes as well as to induce haematopoietic dysplasia in mice and invasive melanomas in p53−/− zebrafish (Davies *et al*., 2002; Ikenoue *et al*., 2004; Wellbrock *et al*., 2004b; Mercer *et al*., 2005; Patton *et al*., 2005). Likewise, suppression of *BRAF*^{V600E} expression in melanoma lines abrogates their transformed phenotype (Hingorani *et al*., 2003; Karasarides *et al*., 2004). However, little is known about the requirements of the B-Raf^{V600E} oncoprotein to display biological activity. Nevertheless, this knowledge will be of particular importance for the development of selective B-Raf inhibitors. Indeed, the currently unidentified S446 kinase has been suggested to represent a potential therapeutic target in neoplasms with high B-Raf activity (Mercer and Pritchard, 2003).

Given the important role of the N-region for the *in vitro* kinase activity of wild-type B-Raf (B-Raf^{wt}), we asked to what extent the charged N-region contributes to the biological activity of B-Raf^{wt} and B-Raf^{V600E}. To this end, we focused our analyses on the impact of B-Raf^{V600E} and mutants thereof on several biological end points rather than by relying exclusively on their catalytic activity measured by immunocomplex *in vitro* kinase assays. This is of particular importance, as the high basal activity that is displayed by B-Raf in such assays does not necessarily reflect its *in vivo* potential to activate the ERK pathway or other biological end points (for a discussion, see MacNicol *et al*., 2000; Mercer and Pritchard, 2003). Here, we show that the N-region is indeed important for the biological activity of B-Raf^{wt} as it opposes negative regulatory constraints probably imposed by 14-3-3 binding to the CR2 domain. This necessity, however, is strongly reduced in B-Raf^{V600E}. Furthermore, we show that the biological activity of B-Raf^{V600E} is independent of its interaction with Ras-GTP.

Results

Comparison of B-Raf^{wt} and B-Raf^{V600E} for their requirement for a negatively charged N-region and Ras-GTP binding to activate the ERK pathway

In view of the high transforming activities of B-Raf^{V600E}, we asked as to whether this oncoprotein still requires a negatively charged N-region or interaction with Ras-GTP. To this end, we introduced the V600E mutation into the pFlu/B-Raf vector encoding N-terminal, hemagglutinine (HA)-tagged chicken B-Raf^{wt}, which is 93% identical with human B-Raf at the amino-acid level (Figure 1a; Brummer *et al*., 2003). To investigate the effect of the V600E mutation on Ras-binding deficient B-Raf, we also introduced this mutation into a vector encoding Ras-GTP binding-deficient B-Raf^{R188L}. In addition, expression vectors encoding either B-Raf or B-Raf^{V600E} with S446/447 replaced by alanine residues were generated (B-Raf$^{S446/7A}$). Lastly, the entire SSDD sequence was mutated to alanine residues to express B-Raf proteins with a completely neutralized N-region (Figure 1a; B-Raf^{Nn}, B-Raf$^{Nn/V600E}$ and B-Raf$^{R188L/Nn/V600E}$). To test whether these B-Raf mutants could be efficiently expressed and were able to activate the ERK pathway, HEK293/EBNA-2 cells were transfected with the aforementioned vectors. The pFlu/B-Raf^{K483W} vector encoding catalytically inactive B-Raf was also included in the study as a negative control. All B-Raf proteins were expressed at comparable levels (Figure 1b) and S446A mutants lacked anti-phospho-S446 reactivity as would be expected. Interestingly, B-Raf^{K483W} was still detected by this antibody (Figure 1b, lane 10), demonstrating that S446 does not represent an autophosphorylation site. Longer exposure revealed that endogenous B-Raf was also phosphorylated at S446 (data not shown), which is in agreement with previous studies conducted in several cell types including HEK293 cells (Mason *et al*., 1999; Brummer *et al*., 2002; Tran *et al*., 2005). Expression of B-Raf^{wt} led to a low level of ERK phosphorylation, whereas B-Raf^{V600E} provoked robust ERK activation as was reported for myc-tagged human B-Raf^{V600E} in COS cells (Davies *et al*., 2002; Wan *et al*., 2004). Compared to B-Raf^{wt}-expressing cells, B-Raf^{R188L}, Raf$^{S446/7A}$, B-Raf^{Nn} or B-Raf^{K483W} transfectants consistently exhibited reduced or undetectable ERK1/2 phosphorylation, indicating that these mutations compromise the activity of B-Raf *in vivo* (Figure 1b and Table 1). However, cells expressing B-Raf$^{R188L/V600E}$, B-Raf$^{S446/7A/V600E}$ and B-Raf$^{Nn/V600E}$ displayed high ERK phosphorylation (Figure 1b), indicating that, at least in this experimental system, the V600E mutation confers an enhanced signalling potential to B-Raf, regardless of the ability of B-Raf to interact with Ras-GTP or the presence of N-region charge.

Table 1 Quantification of ERK phosphorylation induced by B-Raf^{wt} and its RBD and N-region mutants in HEK293/EBNA-2 and Phoenix cells

	HEK293/EBNA-2	*HEK293/Phoenix*
wt	100	100
R188L	68	41
S446/7A	45	36
Nn	36	29

The intensity of ERK phosphorylation was assessed by densitometry and normalized according to the loading control and the relative expression level of HA-tagged B-Raf proteins. The results of two independent experiments, one performed in HEK293/EBNA-2 cells (see Figure 1b) using pFlu/B-Raf vectors and one performed in HEK293/Phoenix cells using pMIG/B-Raf vectors, are shown. The ERK phosphorylation intensity observed in B-Raf^{wt}-expressing cells was set to 100%. Abbreviations: ERK, extracellular signal regulated kinase; HA, hemagglutinine; RBD, Ras-GTP-binding domain.

Comparison of the biological activity of B-Raf^{wt} and B-Raf^{V600E}

Next, we asked to what extent these B-Raf mutants could provoke neuronal differentiation of PC12 cells, a well-established model system to assay Raf mutants for their biological activity (MacNicol *et al*., 2000; Zhang

and Guan, 2000; Dhillon *et al*., 2003). As we have shown previously (Brummer *et al*., 2003), expression of B-Raf^{wt}, but not of B-Raf^{K483W}, resulted in the differentiation of 10–20% of transfectants (Figure 2). In line with its high signalling activity (Figure 1b), approximately 50% of PC12 transfectants expressing B-Raf^{V600E} displayed prominent neurites, a percentage that has been also observed upon expression of other Raf oncogenes (MacNicol *et al*., 2000; Dhillon *et al*., 2003) or the constitutively active enhanced green fluorescent protein (EGFP)-ΔB-Raf protein (Figure 2; Brummer *et al*. 2003). In comparison with B-Raf^{wt} transfectants, those expressing B-Raf^{R188L} displayed a 3–4-fold reduction in neurite outgrowth, indicating that B-Raf must interact with Ras-GTPases to exhibit its full biological activity (Figure 2b). In contrast, PC12 transfectants expressing B-Raf$^{R188L/V600E}$ exhibited prominent neurites to the same extent as those expressing B-Raf^{V600E} indicating that this oncoprotein does not require the interaction with Ras-GTP to induce PC12 differentiation.

Next, we investigated to what extent N-region charge contributes to the biological activity of B-Raf^{wt} and B-Raf^{V600E}. As shown in Figure 2, B-Raf$^{S446/7A}$- and B-Raf^{Nn}-expressing transfectants exhibited a very low degree of differentiation, comparable to that of B-Raf^{K483W}-expressing cells. This demonstrates for the first time the importance of a negatively charged N-region, and in particular of the phosphorylation sites S446/447, for the biological activity of full-length B-Raf. However, the necessity for a negatively charged N-region is rendered obsolete in a B-Raf^{V600E} background as indicated by the biological activity of the corresponding S446/7A and Nn mutants. Furthermore, even the triple B-Raf$^{R188L/Nn/V600E}$ mutant displayed a high differentiative activity (Figure 2b), which also provoked a prominent ERK activity in HEK293 cells (data not shown). It should be also emphasized that at least 700 HA-positive cells (regardless of their staining intensity) were analysed in this assay. Consequently, the obtained result is not weighted on certain B-Raf transgene expression levels. Thus, in the PC12 assay, the V600E gain-of-function mutation dominates over mutations within the SSDD sequence and RBD that compromise the activity of the wild-type protein.

The influence of 14-3-3 binding on the biological activity of B-Raf^{wt} and B-Raf^{V600E}

Next, we asked why N-region phosphorylation is indispensable for the biological activity of B-Raf^{wt}. Recently, it has been suggested that negative charges in the N-region are involved in the maintenance of a more

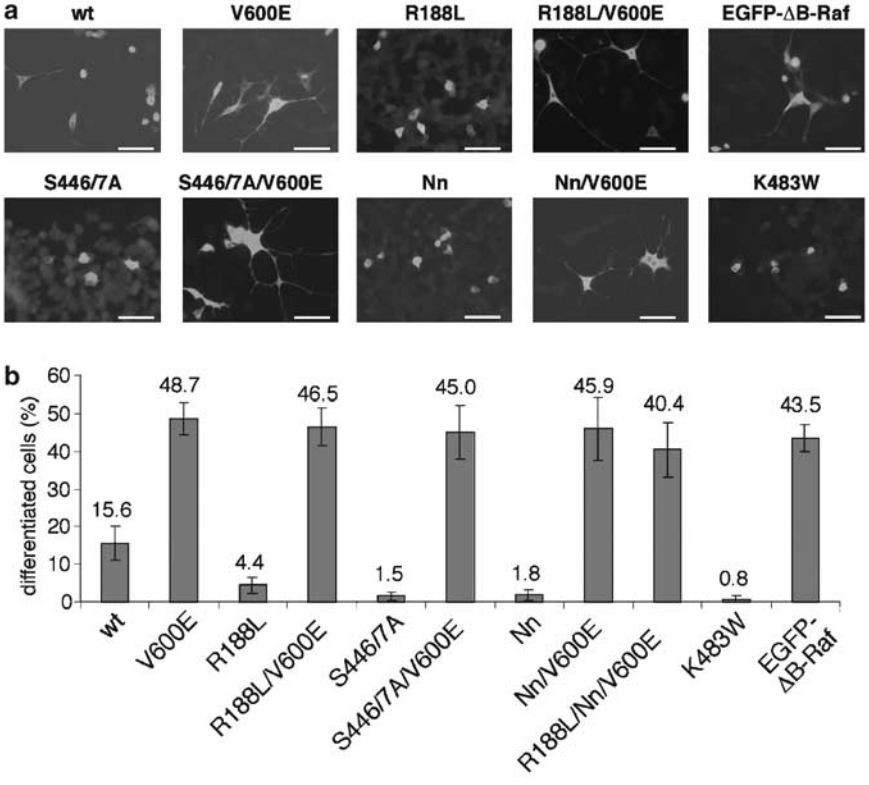

Figure 2 Unlike B-Raf, B-Raf^{V600E} is neither dependent on Ras-GTP nor on a negatively charged N-region to induce PC12 cell differentiation. PC12 cells were transfected with the indicated pFlu/B-Raf plasmids. As a positive and negative control for differentiation, cells were transfected with an expression vector encoding for a constitutively active enhanced green fluorescent protein (EGFP)-ΔB-Raf fusion protein or catalytically inactive B-Raf^{K483W}, respectively (Brummer *et al*., 2003). Transfectants were visualized by immunofluorescence using an anti-hemagglutinine (HA) antibody or GFP fluorescence. (**a**) Representative micrographs. The scale bar corresponds to 50 μM. (**b**) Statistical analysis of differentiation. Each column represents the mean of at least 700 transfectants derived from a minimum of three independent transfections. Standard deviation is indicated by error bars.

open conformation of B-Raf that facilitates the access of activation segment kinases that phosphorylate T599 and S602 (Mercer and Pritchard, 2003). Similarly, Wan *et al*. (2004) have suggested that phospho-S446 may relieve constraints imposed by the N-terminus. Considering these models, we reasoned that the S365A mutation, which should prevent binding of 14-3-3 to the CR2, would rescue the impaired biological activity of B-Raf$^{S446/7A}$. As binding of 14-3-3 proteins to the CR2 has been only confirmed for Raf-1, but not for B-Raf, we first determined whether S365 is indeed involved in 14-3-3 binding. As S729 of B-Raf is a known 14-3-3 recruitment site (MacNicol *et al*., 2000), we performed alanine substitutions of S365 and S729, singly and in combination. Many 14-3-3 client proteins possess more than one 14-3-3 binding site and in this case, it is necessary to eliminate both binding sites to observe an altered stoichiometry of the 14-3-3/client protein complex (Yaffe, 2002). Indeed, mutation of both sites was required to achieve a drastic reduction of the B-Raf/14-3-3 interaction (Figure 3a). Therefore, both S365 and S729 contribute to binding and, at least under these experimental conditions, the third potential 14-3-3 binding site within the cysteine-rich domain of CR1 (Hekman *et al*., 2004) appears not to be a major mediator of 14-3-3/B-Raf interaction.

We then investigated whether the S365A mutation alters the biological activity of B-Raf proteins with or without a neutralized N-region. In the PC12 assay, the S365A mutation markedly enhanced the biological activity of B-Raf (Figure 3b), indicating for the first time that S365 kinases, for example, Akt or SGK (Zhang *et al*., 2001), serve as potent negative regulators of B-Raf in a biological system. However, the differentiative potential of HA-B-Raf^{S365A} did not reach that of B-Raf^{V600E} (Figure 3b), indicating that biological readouts such as 'cellular' MEK/ERK phosphorylation (Figure 3c/d) and PC12 differentiation are appropriate tools to evaluate the activities of B-Raf proteins. It should be also noted that the S365A mutation did not further increase the high biological activity of B-Raf^{V600E} in the PC12 assay (data not shown). Importantly, the presence of the S365A mutation in B-Raf$^{S446/7A}$ rescued the detrimental effect of the S446/447A mutation in the PC12 cell assay (Figure 3b). Furthermore, in a preliminary experiment, the S365A mutation also rescued the impaired biological activity of B-Raf^{Nn}: B-Raf^{wt}: 16.3%; B-Raf^{Nn}: 0.3%; B-Raf$^{S365A/Nn}$: 24.0%; B-Raf$^{Nn/V600E}$: 51.3% (percentages indicate differentiated cells obtained in this experiment; $n = 300$ hemeagglutinine-positive transfectants). The S365A mutation also elevated the MEK/ERK activation potential of B-Raf, but not as dramatically as V600E and this effect was progressively reduced when S365A was combined with S446/7A or a completely neutralized N-region (Figure 3c). MacNicol *et al*. (2000) have demonstrated that the S729A mutation blocks the high biological activity of the isolated B-Raf CR3 while having only a moderate impact on its *in vitro* kinase activity. In agreement with this, we show that the enhanced cellular MEK kinase activity of B-Raf^{S365A} was abolished upon introduction of the S729A mutation, demonstrating that this C-terminal 14-3-3 binding site is essential for the coupling of B-Raf to downstream effectors (Figure 3d). Taken together, these data suggest that one function of the negatively charged N-region is to oppose the stabilization of a closed B-Raf conformation by 14-3-3 binding to phospho-S365. Interestingly, these results also highlight another isoform-specific difference between B-Raf and Raf-1 as Light *et al*. (2002) have shown that the S259A mutation does not rescue the impaired kinase activity of Raf-1^{S338A}.

Determination of the in vitro *kinase activity of B-Raf mutants*

Next, we determined the *in vitro* kinase activities of the aforementioned B-Raf mutants. To this end, we used a coupled *in vitro* kinase cascade assay system (Alessi *et al*., 1995), in which immunopurified HA-B-Raf phosphorylates GST-MEK that in turn activates GST-ERK2. The activation of GST-ERK2 is then assayed using myelin basic protein (MBP) as a substrate in the presence of radioactive ATP. During these experiments, however, we experienced a high background phosphorylation of MBP (data not shown). In contrast, we found that the measurement of phosphorylated GST-MEK1 using a phospho-specific antibody recognizing the amino-acid residues S217 and S221, which are specifically phosphorylated by Raf, provided a more dynamic range. In order to compare the *in vitro* kinase assay results with the pMEK/pERK data from our previous assays (Figures 1b and 3c/d), we immunoprecipitated the various B-Raf proteins from Phoenix-eco cells grown in the presence of serum. Despite its crippled biological activity in PC12 (Figure 2) and Raf-deficient DT40 B cells (Brummer *et al*., 2002), the B-Raf^{R188L} mutant displayed an *in vitro* kinase activity comparable to B-Raf^{wt}, in agreement with the observations of Marais *et al*. (1997). Similar to Mason *et al*. (1999), we also observed a reduction of the activity of B-Raf^{wt} proteins with a partial or neutralized N-region in some experiments, although this result could not be reproduced in all experiments as indicated by the comprehensive analysis in Figure 4a. As reported previously, B-Raf^{V600E} displayed a robust MEK kinase activity, which was about 10-fold higher than that of B-Raf^{wt}, a differential that has also been observed by other laboratories (Davies *et al*., 2002; Ikenoue *et al*., 2003, 2004; Grbovic *et al*., 2006). As expected from the aforementioned experiments in HEK293 and PC12 cells, this high activity was not considerably influenced by the R188L or S446/7A mutations. Interestingly, however, the B-Raf$^{Nn/V600E}$ mutant displayed a 2.5-fold reduction in activity, indicating that the D448/449 residues contribute to the high *in vitro* kinase activity of B-Raf^{V600E} proteins (Figure 4), a difference that was not detected using PC12 cell differentiation and cellular ERK phosphorylation as read-outs. Furthermore, the *in vitro* kinase activity of B-Raf^{S365A} was comparable to that of B-Raf^{V600E} and about twofold more active than the B-Raf$^{Nn/V600E}$ mutant (Figure 4), although both

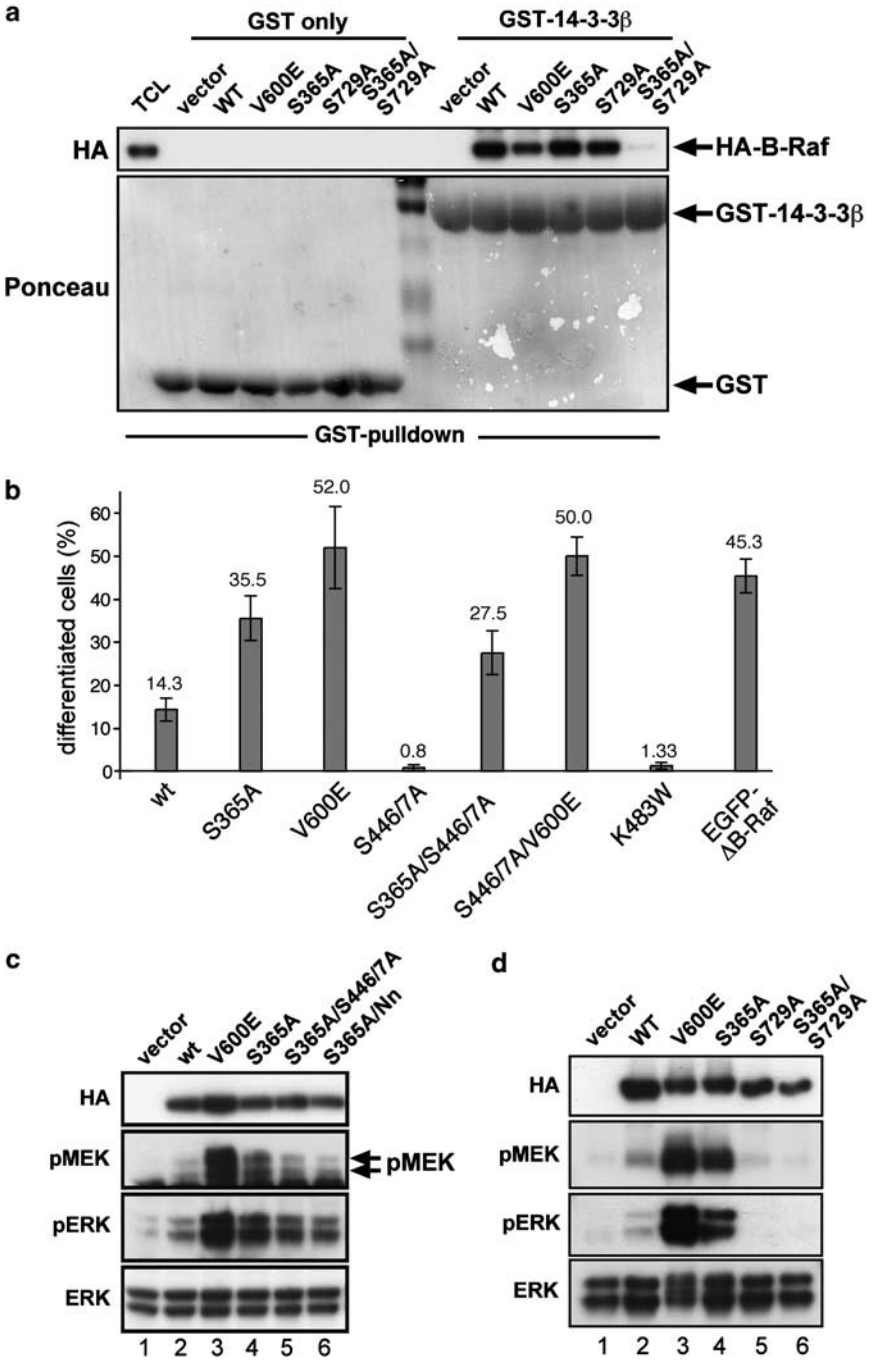

Figure 3 Positive and negative regulation of cellular B-Raf activity by 14-3-3 binding. (**a**) Confirmation of S365 as a 14-3-3 binding site. Hemagglutinine (HA)-B-Raf proteins were expressed in Phoenix-eco cells by transfection with the indicated pMIG vectors and subjected to pull-down analysis using either glutathione-*S*-transferase (GST) (as negative control) or GST-14-3-3β proteins. A protein size marker (visible on the Ponceau-stained membrane) was loaded in the lane between the GST only and GST-13-3-3β pull-down samples. Co-purified HA-tagged B-Raf proteins were detected by Western Blotting using an anti-HA rat monoclonal antibody (upper panel). A total cellular lysate (TCL) containing B-Raf^{wt} was loaded in the first lane on the left-hand side as a positive control. Equal input of GST proteins was verified by Ponceau staining of the polyvinylidine difluoride (PVDF) membrane after Western transfer. Similar expression levels of all B-Raf proteins in the TCLs used for the pulldown experiment were confirmed by Western blot analysis. (**d**). A representative example from three independent experiments is shown. (**b**) Introduction of the S365A mutation rescues the impaired biological activity of B-Raf mutants lacking the serine residues of the N-region. PC12 cells transfected with the indicated plasmids were identified as described in Figure 2. Each column represents the mean of at least 600 transfectants derived from two independent transfections (each performed in triplicate). Standard deviation is indicated by error bars. (**c**) Determination of the MEK/ERK activation potential of B-Raf^{S365A} proteins with a neutralized N-region. Total cellular lysates of Phoenix cells transfected with the indicated pMIG/B-Raf plasmids were subject to a Western blot analysis using the indicated antibodies. (**d**) The C-terminal 14-3-3 binding site is required for optimal cellular B-Raf activity. Total cellular lysates used for the GST-14-3-3 pulldown experiment in (**a**) were subject to a Western blot analyis using the indicated antibodies.

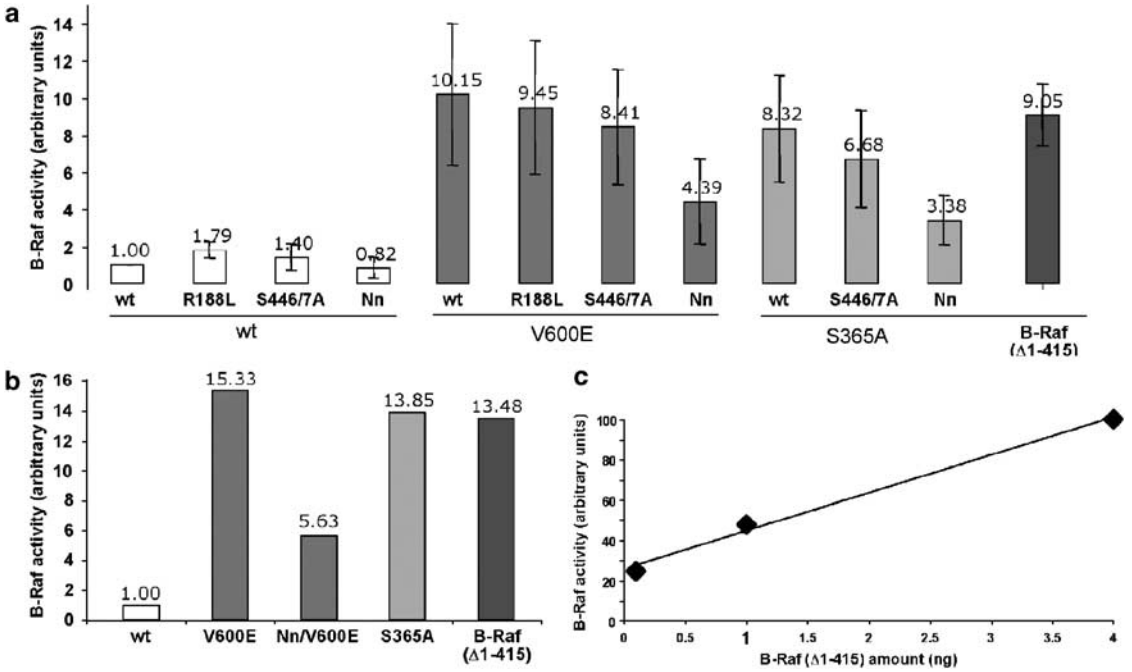

Figure 4 *In vitro* kinase analysis of the B-Raf proteins used in this study. Phoenix-eco cells were transfected with the indicated pMIG/B-Raf constructs. After 48 h, the hemagglutinine (HA)-tagged B-Raf proteins were immunoprecipitated, diluted and subject to an *in vitro* kinase assay as described under Materials and methods. (**a**) *In vitro* kinase activity at 130 μM ATP. Results are the mean of at least three independent kinase reactions derived from at least three independent transfections/immunoprecipitations. In total, 1 ng of active, N-terminally truncated human B-Raf Δ1–415 was used as a positive control. (**b**) *In vitro* kinase activity at 5 mM ATP. A representative experiment out of two independent transfections/immunoprecipitations is shown. (**c**) The *in vitro* kinase assays were performed under non-saturating conditions. Different amounts of B-Raf protein Δ1–415, which correspond to 0.1, 1 and 4 ng of activated B-Raf, were subject to an *in vitro* kinase assay at an ATP concentration of 5 mM as described under Materials and methods. The amount of glutathione-*S*-transferase (GST)-MEK phosphorylation was plotted against the amount of B-Raf Δ1–415.

B-Raf^{V600E} proteins were clearly more active in biological assays (Figures 3b/c/d, 6 and 7). The activity of B-Raf^{S365A} was also progressively reduced by the partial and complete neutralization of the SSDD sequence.

Recently, Wan *et al*. (2004) reported a 500-fold differential between the *in vitro* kinase activities of B-Raf^{wt} and B-Raf^{V600E}, which they attributed to their use of a more physiological ATP concentration of 5 mM. This contrasts with the ATP concentration of 100–800 μM used for the assays in Figure 4a and the aforementioned publications. Therefore, we have repeated the *in vitro* kinase assay with B-Raf^{wt} and the key mutants B-Raf^{V600E}, B-Raf$^{Nn/V600E}$ and B-Raf^{S365A} at 5 mM ATP. This increased ATP concentration had no significant effect on the differential between B-Raf^{wt} and the B-Raf mutants in question (Figure 4b), showing that, under our experimental conditions, the ATP concentration of 130 μM does not limit the activity of B-Raf^{V600E}. Furthermore, using different amounts of activated B-Raf (Δ1–415), we could demonstrate that 1 ng of this protein, which was used as positive control in Figure 4a/b and displays a comparable activity to B-Raf^{V600E}, does not saturate the kinase assay (Figure 4c). A possible explanation for the contrasting differential between B-Raf^{wt} and B-Raf^{V600E} in our study and that of Wan *et al*. (2004) is that we used RIPA buffer for our immunoprecipitations, whereas the latter utilized more mild conditions (0.5% NP-40). Whereas our conditions are probably more specific for B-Raf (by reducing the risk of contamination with other MEK kinases such as Raf-1 (Garnett *et al*., 2005)), they may lead to the dissociation of important cofactors such as the HSP90/p50cdc37 complex (Grammatikakis *et al*., 1999; Grbovic *et al*., 2006).

N-region charge and Ras-GTP binding are dispensable for the transforming potential of B-Raf^{V600E}

We next analysed the potential of B-Raf^{V600E} proteins with a neutralized N-region or a defective RBD to induce oncogenic transformation. To this end, we infected low passage MCF-10A cells with ecotropic retroviruses encoding the indicated B-Raf protein and green fluorescent protein (GFP) (as infection marker) from a bicistronic transcript. MCF-10A cells are immortalized but non-transformed human mammary epithelial cells that form a regular, cobblestone-like monolayer indicating an intact contact inhibition response. As shown in Figure 5, MCF-10A cells expressing only GFP (vector) or the non-V600E B-Raf proteins displayed the typical epithelial phenotype and were well integrated into the growth-arrested monolayer. In contrast, oncogenic Ha-RasG12V (positive control for transformation) and B-Raf^{V600E}-expressing cells exhibited classical features of a transformed phenotype as they lost contact inhibition and grew out

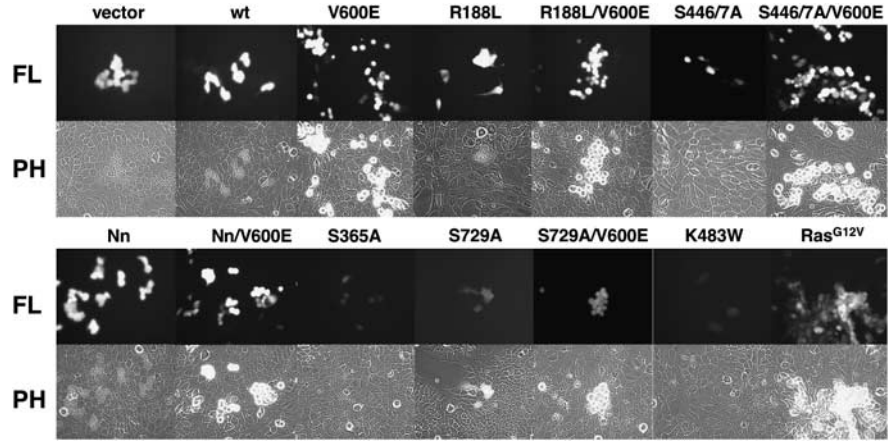

Figure 5 Expression of B-Raf^{V600E} proteins abolishes the contact inhibition response of MCF-10A cells. (**a**) MCF-10A/ecoR cells were infected with the indicated bicistronic pMIG/B-Raf retroviral constructs. Cells infected with pMIG/Ha-RasG12V were used as a positive control. Infected pools were grown to confluency and infected cells were visualized by their green fluorescent protein (GFP) expression under a fluorescence microscope (FL). The same field is also shown in phase contrast microscopy (PH). Note that GFP-positive cells expressing B-Raf^{V600E} or any mutant thereof were no longer contact-inhibited and grew out of the monolayer. Similar results were obtained in at least two independent infection experiments.

of the dense monolayer of non-infected cells as loose clusters of rounded cells that could be easily detached from the monolayer by shearing forces (Figure 5). Importantly, this transforming potential was maintained upon introduction of mutations neutralizing the N-region or abrogating Ras-GTP/B-Raf interaction (Figure 5). Furthermore, although introduction of the S729A mutation reduced the ability of B-Raf^{S365A} to activate MEK/ERK (Figure 3d), expression of B-Raf$^{V600E/S729A}$ was still transforming. As expected from the findings in MCF-10A cells, expression of B-Raf^{V600E} (or its N-region or RBD mutants) in murine NIH 3T3 cells also resulted in a transformed phenotype as indicated by the appearance of refractile cells devoid of any contact inhibition response (data not shown). Thus, the transforming potential of B-Raf^{V600E} is not affected by mutations neutralizing N-region charge or preventing the interaction with Ras-GTP.

Expression of B-Raf^{V600E} induces epithelial–mesenchymal transition in MCF-10A cells

Given the aforementioned findings and the involvement of *BRAF* mutations in particular cancers of epithelial origin, we were interested in the ability of B-Raf^{V600E} and mutants thereof to influence the epithelial morphogenesis programme of MCF-10A cells. First, we analysed whether B-Raf^{V600E} affects the morphology of MCF-10A cells maintained at low density. Non-infected or empty vector-infected MCF-10A cells grew as clusters of cells in close contact and with strong cell–substratum adhesion (Figure 6a). Similarly, MCF-10A cells expressing B-Raf^{wt}, B-Raf^{R188L}, B-Raf^{S365A}, B-Raf^{S729A}, B-Raf^{K483W} and the N-region mutants maintained this epithelial phenotype. In contrast, expression of B-Raf^{V600E} or its mutants led to cells with an elongated, spindle-like morphology that also displayed criss-cross growth, scattering, loss of cell–cell contacts and a strongly reduced cell–substratum interaction (Figure 6a).

When grown in three-dimensional (3D) matrigel cultures, MCF-10A cells undergo a series of proliferative and morphogenetic events leading to the formation of growth-arrested acini-like spheroids composed of a single layer of polarized epithelial cells surrounding a hollow lumen (Debnath *et al*., 2002; Brummer *et al*., 2006). We were therefore interested in analysing the effect of B-Raf and its mutants on this morphogenetic process. MCF-10A cells expressing B-Raf^{wt} and corresponding non-V600E mutants including active B-Raf^{S365A} formed regular acini at day 10 (Figure 6b). In marked contrast, colonies expressing B-Raf^{V600E} or any of its mutants formed 'grape-like' colonies of individual, dis-cohesive cells growing in loose contact that displayed a strong reduction in total β-Catenin staining (Figure 6b), most likely as a result of the loss of membraneous E-Cadherin (Figure 6c). Our bi-cistronic approach and the fact that we used an unsorted pool of MCF-10A cells with varying GFP expression levels for the 3D matrigel culture assays also allowed us to correlate the degree of β-Catenin reduction in individual cells/colonies with the GFP (B-Raf) expression level. This analysis revealed that all GFP-positive cells/colonies expressing B-Raf^{V600E} oncoproteins displayed an aberrant morphology and a strong reduction in β-Catenin staining, demonstrating that these phenotypic changes are not confined to cells with high expression levels of B-Raf^{V600E} or B-Raf$^{Nn/V600E}$, but can be observed at low expression levels as well (Figure 7).

The findings from the matrigel cultures and the morphology observed in monolayer culture suggested that MCF-10A cells expressing B-Raf^{V600E} proteins undergo epithelial–mesenchymal transition (EMT). In order to investigate this further, we subjected RIPA-buffer lysates of the MCF-10A pools to Western Blot analysis using antibodies for E-Cadherin (epithelial

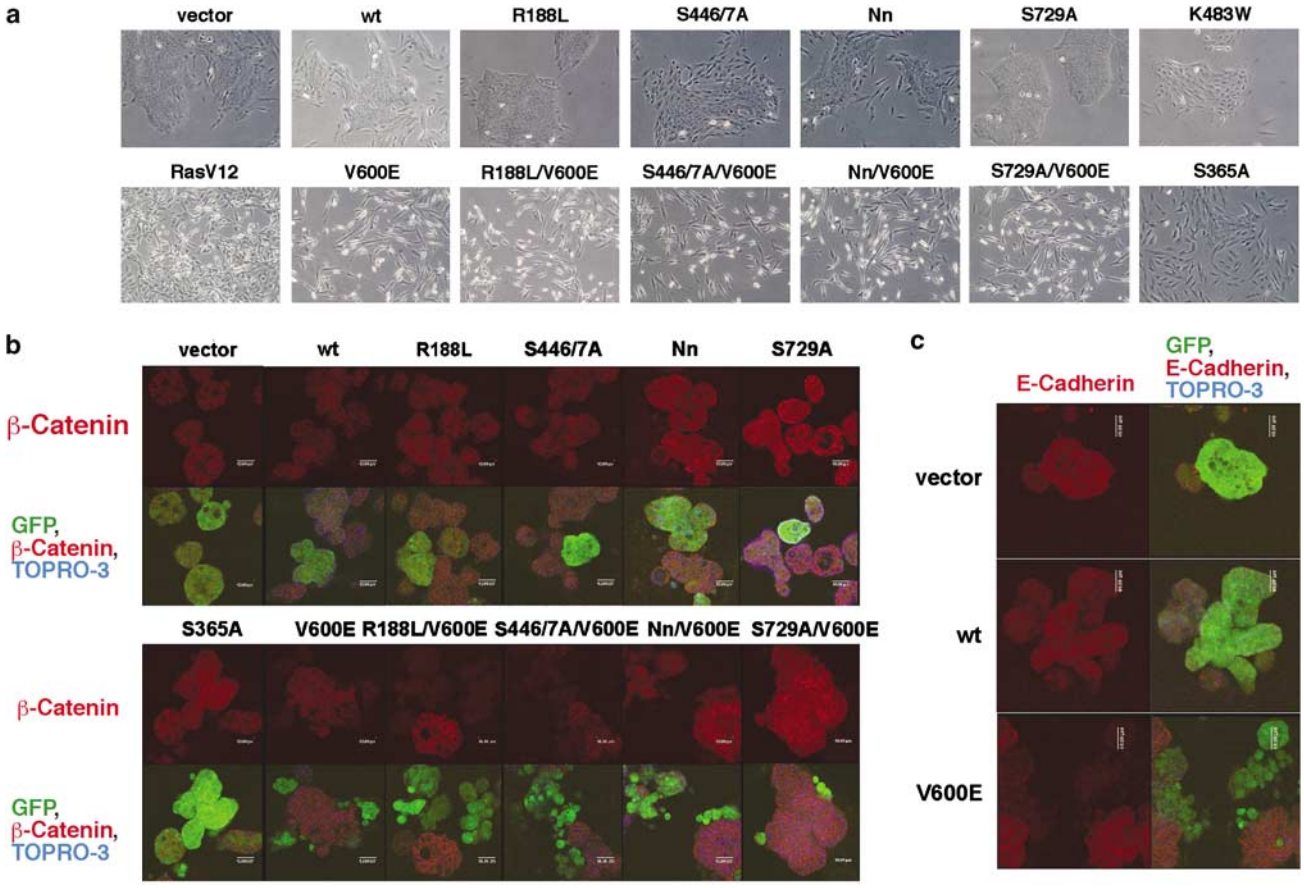

Figure 6 Mutations of the Ras-GTP-binding domain (RBD) and the N-region do not affect the capacity of B-Raf^{V600E} to induce epithelial–mesenchymal transition (EMT) in MCF-10A cells. (**a**) B-Raf^{V600E} induces a fibroblast-like morphology in MCF-10A cells. Stable pools of MCF-10A/ecoR cells infected with the indicated bicistronic retroviral constructs were plated out at low density. After 4 days, their morphology was assessed by phase contrast microscopy. MCF-10A/ecoR cells expressing Ha-RasG12V served as a positive control for EMT induction. Similar results were obtained in at least two independent infection experiments. (**b**) B-Raf^{V600E} disrupts the epithelial morphogenesis programme of MCF-10A cells. Pools of MCF-10A cells infected with the indicated bicistronic retroviruses were seeded into 3D-Matrigel cultures and grown for additional 10 days. Colonies were stained with anti-β-Catenin (Cy-3; red) and TOPRO-3 (blue) as a DNA counter-stain. Expression of the B-Raf-internal ribosomal entry site (IRES)-enhanced green fluorescent protein (EGFP) transcript was indirectly monitored by GFP fluorescence. Green fluorescent protein-negative cells served as an internal control for β-Catenin localization and normal acinar morphogenesis. (**c**) B-Raf^{V600E} expression is correlated with loss of plasma membrane-bound E-cadherin. The experiment was set-up as in (**b**). Colonies were stained with anti-E-Cadherin (Cy-3; red) and TOPRO-3 (blue) as a DNA counter-stain.

marker) and vimentin (mesenchymal marker). This revealed that MCF-10A pools expressing B-Raf^{V600E} exhibited markedly reduced E-Cadherin expression and prominent upregulation of vimentin, whereas B-Raf^{wt}-expressing cells maintained their epithelial characteristics (Figure 8). Furthermore, expression of B-Raf^{V600E} proteins led to a reduction in β-Catenin expression, most likely owing to the loss of its membranous anchorage. As in our previous assays, the S446/7A, Nn- and R188L mutations that attenuate the biological activity of B-Raf^{wt} failed to halt EMT induced by the V600E mutants (Figures 6, 7 and 8a). Also, as observed in HEK293/EBNA-2 transfectants (Figure 1b), expression of all V600E mutants induced a comparable and robust ERK activation. In light of our finding that the S729A mutation blunts the cellular MEK/ERK activation potential introduced by the S365A mutation (Figure 3d), we were surprised to see that the B-Raf$^{V600E/S729A}$ mutant still provokes a prominent ERK activation and EMT (Figure 8b).

Discussion

In this study, we have investigated the requirements for N-region charge, 14-3-3 binding and recruitment to Ras-GTP in the activation and biological activity of B-Raf and its oncogenic counterpart B-Raf^{V600E}. Our findings reveal marked differences in the requirements of these two proteins to achieve their full signalling potential, shed light on the oncogenic potential of B-Raf and provide important information regarding the validity of potential therapeutic approaches directed against B-Raf^{V600E}.

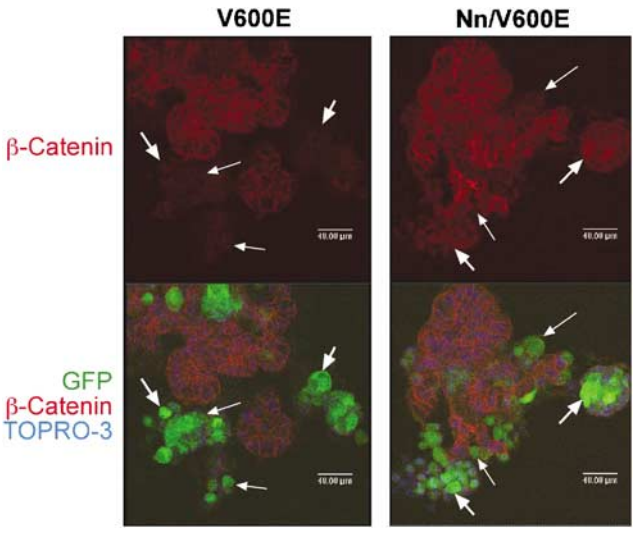

Figure 7 The degree of β-Catenin reduction is not influenced by the expression levels of B-Raf^{V600E} and B-Raf^{V600E}. Pools of MCF-10A cells infected with the indicated bicistronic retroviruses were seeded into 3D-Matrigel cultures, grown for additional 10 days and stained as described in Figure 6b. Expression of the B-Raf-IRES-enhanced green fluorescent protein (EGFP) transcript was indirectly monitored by GFP fluorescence. Bold and thin arrows highlight cells/colonies with high and low GFP(B-Raf) expression, respectively. Note that cells indicated with bold and thin arrows display a comparable reduction in β-Catenin expression (compare upper and lower panel). Green fluorescent protein-negative cells served as an internal control for β-Catenin localization and normal acinar morphogenesis.

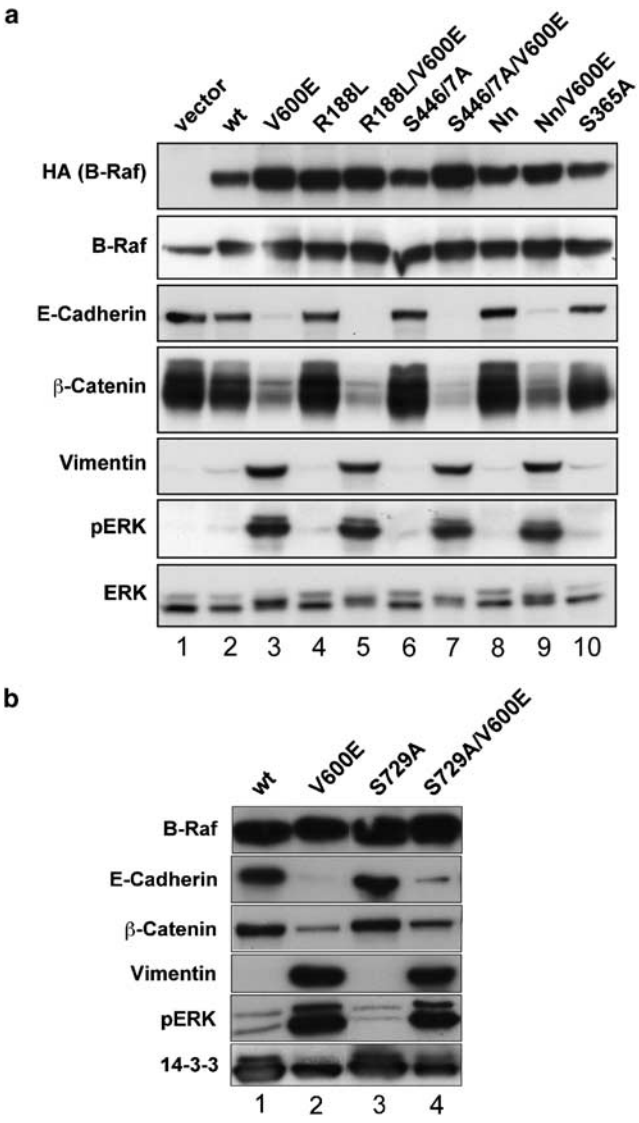

Figure 8 Expression of B-Raf^{V600E} provokes profound changes in the expression of epithelial and mesenchymal marker proteins (**a** and **b**). Total cellular lysates of starved MCF-10A cells infected with the indicated bicistronic retroviruses were subject to Western blot analysis using the indicated antibodies. The expression of exogenous B-Raf was monitored by blotting with an anti-HA antibody. The degree of B-Raf overexpression can be deduced from the anti-B-Raf blot (second panel from top) showing total B-Raf (endogenous B-Raf and HA-tagged B-Raf). The densitometric analysis of a non-saturated exposure of this anti-B-Raf detection revealed that the HA-B-Raf proteins were on average 10-fold overexpressed over endogenous B-Raf. Detection of pERK reveals the extent of B-Raf-mediated extracellular signal regulated kinase (ERK) activation. Detection of total ERK (**a**) and 14-3-3 proteins (**b**) serve as loading control. Similar results were obtained in three independent experiments performed with cell pools derived from at least two independent infections.

B-Raf proteins with a partially or completely neutralized N-region display a lower signalling potential and are impaired in their ability to induce PC12 differentiation, demonstrating for the first time an important role for the negatively charged N-region in the biological activity of full-length B-Raf^{wt} (Figures 1 and 2). However, what is the role of the N-region in the activation of B-Raf^{wt}? According to our current model, B-Raf is primed for activation by constitutive S446 phosphorylation prior to the interaction with Ras-GTP (Brummer *et al*., 2002). The phosphorylation of S446 (and perhaps S447) leads to a maximal negatively charged N-region, which induces a conformational change rendering the activation segment more accessible to its cognate kinase. Our finding that the S365A mutation increases not only the biological activity of B-Raf^{wt} but also rescues that of B-Raf with a neutralized N-region (Figure 3b and c) strongly supports a model in which a major function of the N-region is to oppose the transition into an inactive conformation stabilized by binding of a 14-3-3 dimer to S365 and S729. Our model (Figure 9a), similar to that suggested by Mercer and Pritchard (2003), is consistent with recent studies showing that the negatively charged N-region of Raf-1 relieves autoinhibition by the N-terminal moiety owing to its reduced affinity towards a CR3 with a charged N-region (Cutler *et al*., 1998; Tran and Frost, 2003). However, we accept that similar experiments led to the alternative conclusion that the charged N-region induces a conformational change that does not affect the interaction between N- and C-terminal moiety but renders the CR3 resistant to the autoinhibition imposed by the N-terminal moiety (Chong and Guan, 2003). Furthermore, while our manuscript was in preparation, Tran *et al*. (2005) reported that introduction of the

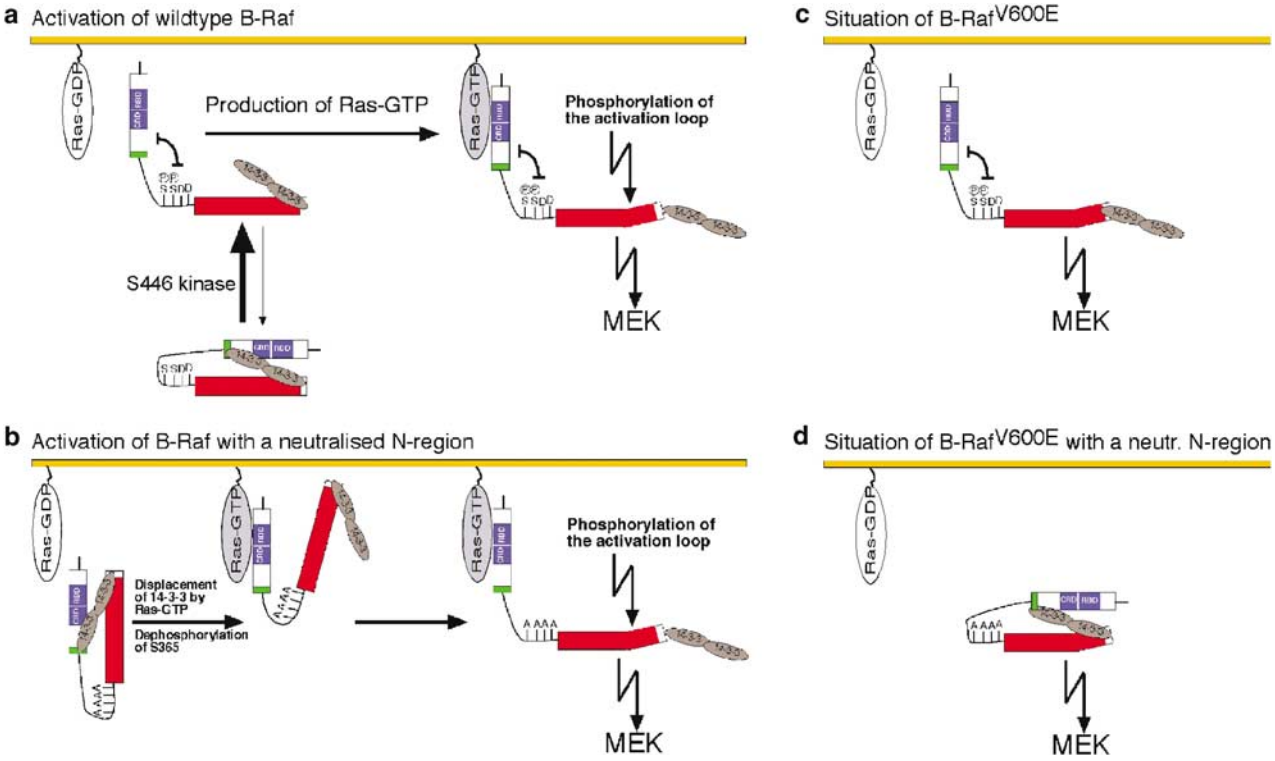

Figure 9 Sequential model of B-Raf activation. (**a**) Situation of wild-type B-Raf. B-Raf is primed for activation by phosphorylation at S446 prior to its interaction with Ras-guanine 5′-triphosphate (GTP). This leads to a maximally negatively charged N-region, which confers an open activation-competent conformation to B-Raf by opposing the closed conformation mediated by simultaneous binding of a 14-3-3 dimer to phosphorylated S365 and S729. Presumably, this open conformation of B-Raf that is achieved prior to interaction with Ras-GTP also explains why it binds MEK-1 with higher affinity than Raf-1 (Papin *et al*., 1998). Induction of Ras-GTP by extracellular signals results in the recruitment of pre-activated B-Raf to the plasma membrane where it is fully activated by activation segment kinases. This assumption is supported by the observation that a membrane-targeted B-Raf-CAAX protein displays constitutive MAPKKK and high transforming activities (Papin *et al*., 1998; Carey *et al*., 2003). Phosphorylation of the activation segment destabilizes the inactive conformation of the kinase domain (Wan *et al*., 2004) and renders B-Raf fully active. (**b**) Situation of B-Raf with a neutralized N-region. If the N-region is neutralized, most B-Raf molecules will reside in a closed, inactive conformation stabilized by 14-3-3 proteins binding to S365 and S729. Only upon Ras-GTP binding is the 14-3-3 dimer displaced from S365, switching B-Raf into a more open conformation permitting phosphorylation and the conformational change of the activation segment. If this last step is mimicked by the V600E mutation, the preceding steps of S446 phosphorylation and interaction with Ras-GTP are superfluous (**c**, **d**).

S446A mutation into the isolated CR3 increased the affinity of this region towards the isolated N-terminal domain of B-Raf (Tran *et al*., 2005). Therefore, these and our data provide strong evidence for a model wherein an important function of phospho-S446 is to relieve the autoinhibition imposed by the N-terminal region of B-Raf. In this regard, the charged N-region may recruit proteins that stabilize this 'primed' conformation. Such proteins might also protect the N-region against phosphatases and could provide an explanation for the constitutive S446 phosphorylation of B-Raf that is observed in different cell types and species. Indeed, recent findings have shown that the adapter protein CNK1 binds to Raf-1 in an inducible and Ras-GTP-dependent manner, whereas its association with B-Raf and pre-activated Raf-1 mutants with increased N-region charge is constitutive and Ras-GTP independent (Ziogas *et al*., 2005). Thus, proteins like CNK1 may assist in the stabilization of the primed state. The charged N-region is also likely to stabilize the active conformation of the kinase domain through a salt-bridge between D^{448} and R^{506} (Wan *et al*., 2004). This second important function is likely to explain the different *in vitro* kinase activities between S446/7A and Nn mutants (Figure 4a/b). Thus, the SSDD motif might serve a double function in B-Raf activation, one to facilitate full activation by membrane-resident activation segment kinases by maintaining a primed conformation and another to stabilize the active conformation of the kinase domain after the activation segment has been phosphorylated.

In the case of $B\text{-}Raf^{V600E}$, introduction of the S446/7A mutations did not affect kinase activity *in vitro*, whereas replacement of the entire SSDD sequence by alanine residues diminished this approximately 2.5-fold, although the activity of the $B\text{-}Raf^{Nn/V600E}$ mutant was still four times higher than that of $B\text{-}Raf^{wt}$ (Figure 4). However, the $B\text{-}Raf^{Nn/V600E}$ mutant displayed comparable biological activity in HEK293 (ERK phosphorylation), PC12 (differentiation) and MCF-10A cells (ERK phosphorylation, transformation and EMT induction) as $B\text{-}Raf^{V600E}$ (Figures 1, 5–8). Similarly, while our

manuscript was under revision, Emuss *et al*. (2005) reported that B-Raf$^{Nn/V600E}$ displayed a strong reduction in its *in vitro* kinase activity but retained a very high transforming activity and induced MEK phosphorylation to a comparable extent as B-Raf^{V600E}. As our study and that of Emuss *et al*. (2005) both involve ectopic expression of the respective proteins, it could be argued that our inability to detect a difference in the biological activity of B-Raf^{V600E} proteins with and without complete N-region charge neutralization could be owing to their levels of expression. Alternatively, the difference between the *in vitro* kinase activities of B-Raf^{V600E} and B-Raf$^{Nn/V600E}$ might represent an artefact of the enzymatic conditions *in vitro* and may not apply to these B-Raf^{V600E} proteins in their native environment where membrane phospholipids and other co-factors are present. Formal resolution of this issue will require germline knock-ins of the V600E mutation, in the presence and absence of the Nn mutations, into the murine B-*raf* locus. Furthermore, our finding that B-Raf^{S365A} displays an *in vitro* kinase activity comparable to B-Raf^{V600E}, but exhibits a reduced ability to activate ERK (Figure 3), induce PC12 cell differentiation (Figure 3) and to promote EMT in MCF-10A cells (Figures 6 and 8), indicates that our *in vivo* assays are capable of discriminating between the biological activities of activated B-Raf proteins. We assume that the contrasting relative activities of B-Raf^{V600E} and B-Raf^{S365A} *in vitro* and *in vivo* reflect the differential sensitivity of these proteins to endogenous negative regulatory factors, for example, RKIP or Sprouty proteins, (Tsavachidou *et al*., 2004; Kolch, 2005), which may be lost during the immunopurification procedure, or the capacity of B-Raf^{V600E} to trigger additional signalling pathways, a property not reflected in the *in vitro* kinase assay employed.

However, if N-region charge opposes a closed, inactive conformation of B-Raf, why are the biological and, to a lesser extent, *in vitro* kinase activities of B-Raf^{V600E} resilient to N-region neutralization? Among several possibilities, we think that this question can be best explained by the model of sequential B-Raf activation (Figure 9). According to the recently published crystal structure, phosphorylation of T599/S602 or the V600E mutation distorts the activation segment in such a way that the inactive conformation that is stabilized by the hydrophobic interaction between V600 in the activation segment and F467 in the glycine-rich loop is disrupted (Hubbard, 2004; Wan *et al*., 2004). If all the priming steps preceding B-Raf^{wt} activation are only required to allow activation segment phosphorylation and a switch of the kinase domain to an active conformation (Figure 8a), these events become superfluous if this final step is mimicked by the V600E activation (Figure 8c/d). Alternatively, as suggested by Wan *et al*. (2004), the glutamic acid residue introduced by the V600E mutation might contact K507 within the Cα-helix and thereby stabilize the active conformation. As the salt-bridge between D448 (and maybe phospho-S446/7) and R506 is also implicated in this process (Garnett and Marais, 2004), the E600/K507 salt-bridge could substitute for the absent N-region/R506 interaction in B-Raf^{V600E} proteins with a neutralized N-region. In order to test this hypothesis, it would be interesting to analyse the requirement of the activated B-Raf$^{V600G/K/M/R}$ mutants (Wan *et al*., 2004) for a charged N-region, as these mutants cannot generate the aforementioned E600/K507 salt-bridge. However, a different explanation must underlie the relatively high *in vitro* kinase activity of the B-Raf$^{S365A/Nn}$ mutant, which is comparable to that of B-Raf$^{Nn/V600E}$ (Figure 4), as the alternative salt-bridge cannot be formed in this protein.

In the present study, we are the first to directly analyse the requirements of B-Raf^{V600E} for Ras-GTP by using the Ras-GTP-binding deficient B-Raf^{R188L} mutant, which is refractory to extracellular signals (Brummer *et al*., 2002) and cannot be recruited to the plasma membrane by Ras (Marais *et al*., 1997). Our analysis of the HA-B-Raf$^{R188L/V600E}$ mutant clearly demonstrates that the biological activity and transforming potential of B-Raf^{V600E} are independent of its ability to interact with Ras-GTP and imply that the V600E mutation circumvents the need for Ras-GTP-stimulated phosphorylation of T599 and S602. Consequently, this finding would also explain why *BRAF*^{V600E} and oncogenic *RAS* alleles are mutually exclusive in cancer types characterized by a high incidence of *RAS* mutations. However, our data do not exclude the possibility that B-Raf^{V600E} induces autocrine loops signalling through Ras-GTPases and such a scenario would also explain why B-Raf^{V600E} requires the presence of isoprenylcysteine-carboylmethyltransferase, an enzyme required for the correct subcellular localization of Ras-GTPases, for full transformation (Bergo *et al*., 2004).

In the present study, we also show for the first time that expression of B-Raf^{V600E} induces EMT of MCF-10A cells. The observed reduction in E-Cadherin expression is presumably owing to chronic ERK activation (Figure 8), which would lead to decreased transcription of the E-Cadherin encoding CDH1 gene via the upregulation of Snail family repressors (Thiery, 2002). Furthermore, loss of E-Cadherin expression was correlated with a strong reduction in β-Catenin expression, presumably, owing to loss of membranous anchorage. The resulting subcellular redistribution of β-Catenin might then increase nuclear β-Catenin signalling, a hypothesis supported by the strong upregulation of the mesenchymal marker and β-Catenin target gene vimentin (Gilles *et al*., 2003). Our findings are of particular interest as aberrant β-Catenin signalling and EMT have been implicated as important processes in the metastatic progression of tumours with a high incidence of *BRAF*^{V600E} mutations such as melanomas, thyroid and colorectal carcinomas (Thiery, 2002). Likewise, as EMT and its opposite process are crucial and tightly regulated events during metazoan development, our finding that B-Raf^{V600E} induces EMT might help to explain the embryonic lethal phenotype of mouse embryos with an induced B-*raf*^{V600E} allele (Mercer *et al*., 2005).

In summary, five fundamental regulatory differences between B-Raf^{wt} and B-Raf^{V600E} have now been identified, as the V600E mutation circumvents the require-

ment for Ras-GTP binding, N-region charge and binding of 14-3-3 to S729 (Figures 1, 2, 5, 6, 7 and 8), and confers resistance to negative feedback regulation by Sprouty proteins (Tsavachidou *et al*., 2004) and the effects of S579A mutation (Zhu *et al*., 2005). Our data suggest that the high biological activity of B-Raf^{V600E} cannot be directly inhibited by compounds interfering with Ras activation or S446 phosphorylation and that the development of therapies for tumours harbouring a *BRAF*^{V600E} allele should focus on the inhibition of the catalytic centre or expression of B-Raf. However, still to be developed S446 kinase inhibitors might be useful for the treatment of pathologies that are dependent on B-Raf signals but contain *BRAF*^{wt} alleles, for example, tumours overexpressing B-Raf^{wt} or harbouring activating mutations of upstream activators such as Ras or receptor tyrosine kinases, or polycystic kidney disease, which is characterized by increased B-Raf activation (Tanami *et al*., 2004; Yamaguchi *et al*., 2004). Similarly, S446 kinase inhibitors might be useful to attenuate the activity of other clinically relevant non-V600E B-Raf mutants. Indeed, recent work by Emuss *et al*. (2005) suggests that this concept might apply to the B-Raf^{E586K} mutant. Thus, unlike many other *BRAF* mutations, the V600E mutation event might be subject to an extraordinary positive selection, because the resulting oncoprotein appears to be particularly independent of key positive regulatory events required for B-Raf^{wt} activation, while also conferring resistance to negative modulation. Thus, our findings also contribute to a better understanding of why this mutation is so frequently found in human tumours.

Materials and methods

Plasmid constructs
The pFlu/B-Raf vector encoding HA-tagged bursal chicken B-Raf has been described (Brummer *et al*., 2003). It should be noted that the recently revised human B-Raf cDNA (Wellbrock *et al*., 2004a) as well as the chicken B-Raf cDNA used in this study (Brummer *et al*., 2003) represent the same splice variant (lacking the neuron-specific exon 10) and are both one amino acid longer than the previously reported human cDNA. Consequently, amino-acid (aa) residues like R187, S364, S445, V599 and S728, which were mentioned throughout earlier publications, correspond in fact to R188, S365, S446, V600 and S729 in both chicken B-Raf and the recently revised human B-Raf (for a review, see Wellbrock *et al*. (2004a)). For the construction of the retroviral vectors, the cDNA was subcloned into the pMIG vector (a kind gift of Dr Warren S Pear) to yield pMIG/B-Raf expressing a bi-cistronic transcript encoding HA-tagged B-Raf and EGFP as an infection marker. Similarly, the Ha-Ras^{G12V} cDNA was subcloned from pCMV5/Ha-Ras^{G12V} (a kind gift of Dr Peter E Shaw) into pMIG. All mutations were introduced using the 'Quick change' site-directed mutagenesis kit (Stratagene).

Transfections, retroviral infections, differentiation and transformation assays
HEK293/EBNA-2 cells (Invitrogen, Paisley, UK) and Phoenix-eco, a HEK293 derivative, and PC12 cells were grown as described (Brummer *et al*., 2003, 2006). Both PC12 cells (5×10^5 cells/35 mm diameter dish) and HEK293/EBNA-2 cells (5×10^5/35 mm diameter dish) were transfected with 3 μg plasmid DNA using 10 μl Gene Juice reagent (Novagen, Schwalbach, Germany) in 3 ml culture medium according to the protocol supplied by the manufacturer. After 3–4 days, PC12 transfectants were identified by positive HA staining and neuronal differentiation was quantified by scoring cells with neurites longer than the size of two cell bodies as described previously (Brummer *et al*., 2003). Phoenix-eco cells were transfected with 10 μg plasmid DNA using Polyfect (Qiagen, Hilden, Germany).

MCF-10A cells expressing the receptor for murine retroviruses (MCF-10A/ecoR; a kind gift of Drs Danielle K Lynch and Joan Brugge) were grown and infected with retroviruses as described (Brummer *et al*., 2006). For biochemical experiments, EGFP-positive cells were sorted by flow cytometry to homogeneity and cultured as pure population. As MCF-10A cells expressing HA-B-Raf^{V600E} (or any mutation thereof) display strongly reduced cell–cell and cell–substrate adhesion, cells infected with pMIG/B-Raf^{V600E} (or any mutation thereof) were isolated by flushing infected cell lawns with growth medium and re-plating of the cells in the supernatant. This method yielded populations highly enriched for EGFP-positive cells. Three-dimensional basement matrigel cultures were set up, maintained, fixed and stained with the indicated antibodies as described (Brummer *et al*., 2006).

Antibodies The anti-phospho-Raf-1 S338 antibody recognizing pS446 was purchased from Upstate Biotechnology, Charlottesville, VA, USA. B-Raf proteins were detected using anti-B-Raf F7 antibody (Santa Cruz, CA, USA). Other antibodies used in this study were anti-E-Cadherin (clone 36) and β-Catenin (clone 14) (both BD Transduction Laboratories, Heidelberg, Germany), anti-Vimentin (Amersham, Castle Hill, NSW, Australia), anti-14-3-3β (recognizes all 14-3-3 isoforms; Santa Cruz), anti-HA antibodies 12CA5 or 3F10 (Roche Molecular Bioscience, Castle Hill, NSW, Australia), anti-ERK2 (Transduction labs) and anti-p42/p44 MAPK (Cell Signaling Technology, Beverly, MA, USA). Phospho-ERK was detected using antiactivated MAPK 12D4 (nanotools) or phospho-MAPK (Cell Signaling Technology, Beverly, MA, USA).

Western blot analysis TCLs were generated and analysed by Western Blotting as described previously (Brummer *et al*., 2004). If not stated otherwise, cells were lysed in RIPA-buffer (50 mM HEPES, pH 7.4; 1% Triton X-100; 0.5% Sodium deoxycholate, 0.1% SDS, 50 mM Sodium fluoride, 5 mM EDTA, supplemented with protease inhibitors (0.1 mg/ml aprotinin, 0.5 mg/ml leupeptin, 1 mM AEBSF or PMSF). Transfectants were directly processed to TCLs without starvation.

In vitro *kinase assays* A B-Raf *in vitro* kinase assay kit (Upstate Biotechnology) was used for the determination of the *in vitro* kinase activities of the various B-Raf proteins. A subconfluent 10 cm dish of Phoenix-eco cells was transfected with 10 μg of the indicated pMIG plasmids as described above and was lysed in 1.5 ml RIPA buffer 48 h post transfection. Subsequently, 0.5–1 μg rat anti-HA antibody 3F10 was added to 1.2 ml cleared TCL for 2 h and then incubated with 50 μl Protein G-Sepharose slurry for 3 h. Following three washes with 1 ml RIPA-buffer and four washes with 1 ml Kinase assay buffer (KAB; 20 mM 4-Morpholinepropanesulfonic acid (MOPS), pH 7.2; 25 mM β-glycerol phosphate; 5 mM EGTA, 1 mM sodium orthovanadate, 1 mM dithiothreitol), the beads were resuspended in 100 μl KAB. Then, 10 μl of this

suspension were mixed with 0.4 μg GST-MEK1, 1 μg GST-ERK2 and supplied 10 μl Mg^{2+}/ATP solution (75 mM $MgCl_2$; 500 μM ATP dissolved in KAB) and KAB added to a final volume of 38 μl. For the *in vitro* kinase assays with a final ATP concentration of 5 mM, the supplied Mg^{2+}/ATP solution was replaced by 10 μl of self-made Mg^{2+}/ATP solution (75 mM $MgCl_2$; 20 μM ATP). The reaction was incubated at 30°C for 30 min and immediately stopped by addition of sample buffer and boiling for 5 min. Subsequently, the reactions were diluted 1:4, separated by SDS–PAGE and blotted with phospho-MEK antibodies as read-out for the MEK kinase activity of the purified HA-B-Raf proteins. The phospho-MEK signal was analysed using IP Lab Gel software (Signal Analytics Corp.). Following subtraction of the background signal (kinase assay reaction performed with anti-HA immunoprecipitates of empty vector-transfected cells), the relative, specific B-Raf activity was determined by division of each activity by that of $B\text{-}Raf^{wt}$. As a positive control, 1 ng of an activated human B-Raf protein (Upstate Biotechnologies) with an N-terminal truncation of amino acids 1–415, which was purified from SF9 cells, was used in a parallel assay as directed by the manufacturer.

Glutathionine-S-transferase fusion protein pulldown assay *Escherichia coli* BL21Lys were transformed with either pGEX-4T (for production of GST, Pharmacia) or pGEX-14-3-3β (a kind gift from Dr John Hancock; (Roy *et al*., 1998)) plasmids. Expression and purification of GST proteins was performed as described previously (Brummer *et al*., 2004). Phoenix cells expressing HA-tagged B-Raf proteins (confluent 10 cm dish) were lysed in ice-cold lysis buffer (1% v/v Triton-X-100, 50 mM HEPES pH 7.5, 150 mM NaCl, 10% v/v glycerol, 1.5 mM $MgCl_2$, 1 mM EGTA, 10 mM sodium pyrophosphate, 1 mM sodium orthovanadate, 1 mM phenylmethylsulphonyl fluoride, 10 μg/ml aprotinin and 10 μg/ml leupeptin). Postnuclear supernatants were incubated overnight with an appropriate volume of GST-fusion proteins (approx. 25 μg) immobilized on glutathionine-Sepharose beads. Subsequently, the beads were washed six times with 1 ml lysis buffer, resuspended in 100 μl lysis buffer, mixed with 50 μl 3 × sample buffer and denatured by boiling for 5 min. The samples were then analysed by Western blotting.

Acknowledgements

We thank Liz Caldon, Drs Alexander Swarbrick and Darren Saunders for advice on the MCF-10A system, Dr Rebecca Newton for cell sorting and Drs Michael Huber and Hassan Jumaa for helpful discussions. We also acknowledge Kate Jeffrey, Drs Prudence Stanford and Paul Timpson for critical reading of the manuscript. This work was supported by the Deutsche Forschungsgemeinschaft through SFB 388 (MR), the National Health and Medical Research Council of Australia and the Cancer Council New South Wales (RJD) as well as the Australian Cancer Research Foundation.

References

Alessi DR, Cohen P, Ashworth A, Cowley S, Leevers SJ, Marshall CJ. (1995). *Methods Enzymol* **255**: 279–290.
Bergo MO, Gavino BJ, Hong C, Beigneux AP, McMahon M, Casey PJ *et al*. (2004). *J Clin Invest* **113**: 539–550.
Brummer T, Elis W, Reth M, Huber M. (2004). *Methods Mol Biol* **271**: 189–212.
Brummer T, Naegele H, Reth M, Misawa Y. (2003). *Oncogene* **22**: 8823–8834.
Brummer T, Schramek D, Hayes VM, Bennett HL, Caldon CE, Musgrove EA *et al*. (2006). *J Biol Chem* **281**: 626–637.
Brummer T, Shaw PE, Reth M, Misawa Y. (2002). *EMBO J* **21**: 5611–5622.
Carey KD, Watson RT, Pessin JE, Stork PJ. (2003). *J Biol Chem* **278**: 3185–3196.
Chong H, Guan KL. (2003). *J Biol Chem* **278**: 36269–36276.
Chong H, Lee J, Guan KL. (2001). *EMBO J* **20**: 3716–3727.
Cutler Jr RE, Stephens RM, Saracino MR, Morrison DK. (1998). *Proc Natl Acad Sci USA* **95**: 9214–9219.
Davies H, Bignell GR, Cox C, Stephens P, Edkins S, Clegg S *et al*. (2002). *Nature* **417**: 949–954.
Debnath J, Mills KR, Collins NL, Reginato MJ, Muthuswamy SK, Brugge JS. (2002). *Cell* **111**: 29–40.
Dhillon AS, Meikle S, Peyssonnaux C, Grindlay J, Kaiser C, Steen H *et al*. (2003). *Mol Cell Biol* **23**: 1983–1993.
Dhillon AS, Meikle S, Yazici Z, Eulitz M, Kolch W. (2002). *EMBO J* **21**: 64–71.
Emuss V, Garnett M, Mason C, Marais R. (2005). *Cancer Res* **65**: 9719–9726.
Garnett MJ, Marais R. (2004). *Cancer Cell* **6**: 313–319.
Garnett MJ, Rana S, Paterson H, Barford D, Marais R. (2005). *Mol Cell* **20**: 963–969.
Gilles C, Polette M, Mestdagt M, Nawrocki-Raby B, Ruggeri P, Birembaut P *et al*. (2003). *Cancer Res* **63**: 2658–2664.
Grammatikakis N, Lin JH, Grammatikakis A, Tsichlis PN, Cochran BH. (1999). *Mol Cell Biol* **19**: 1661–1672.
Grbovic OM, Basso AD, Sawai A, Ye Q, Friedlander P, Solit D *et al*. (2006). *Proc Natl Acad Sci USA* **103**: 57–62.
Harding A, Hsu V, Kornfeld K, Hancock JF. (2003). *J Biol Chem* **278**: 45519–45527.
Hekman M, Wiese S, Metz R, Albert S, Troppmair J, Nickel J *et al*. (2004). *J Biol Chem* **279**: 14074–14086.
Hingorani SR, Jacobetz MA, Robertson GP, Herlyn M, Tuveson DA. (2003). *Cancer Res* **63**: 5198–5202.
Hou XS, Chou TB, Melnick MB, Perrimon N. (1995). *Cell* **81**: 63–71.
Hubbard SR. (2004). *Cell* **116**: 764–766.
Ikenoue T, Hikiba Y, Kanai F, Aragaki J, Tanaka Y, Imamura J *et al*. (2004). *Cancer Res* **64**: 3428–3435.
Ikenoue T, Hikiba Y, Kanai F, Tanaka Y, Imamura J, Imamura T *et al*. (2003). *Cancer Res* **63**: 8132–8137.
Karasarides M, Chiloeches A, Hayward R, Niculescu-Duvaz D, Scanlon I, Friedlos F *et al*. (2004). *Oncogene* **23**: 6292–6298.
Kolch W. (2005). *Nat Rev Mol Cell Biol* **6**: 827–837.
Light Y, Paterson H, Marais R. (2002). *Mol Cell Biol* **22**: 4984–4996.
MacNicol MC, Muslin AJ, MacNicol AM. (2000). *J Biol Chem* **275**: 3803–3809.
Marais R, Light Y, Paterson HF, Mason CS, Marshall CJ. (1997). *J Biol Chem* **272**: 4378–4383.
Mason CS, Springer CJ, Cooper RG, Superti-Furga G, Marshall CJ, Marais R. (1999). *EMBO J* **18**: 2137–2148.
Mercer K, Giblett S, Green S, Lloyd D, Darocha Dias S, Plumb M *et al*. (2005). *Cancer Res* **65**: 11493–11500.
Mercer KE, Pritchard CA. (2003). *Biochim Biophys Acta* **1653**: 25–40.
Morrison DK. (2004). *Nature* **428**: 813–815.
O'Neill E, Kolch W. (2004). *Br J Cancer* **90**: 283–288.
Papin C, Denouel-Galy A, Laugier D, Calothy G, Eychene A. (1998). *J Biol Chem* **273**: 24939–24947.

Patton EE, Widlund HR, Kutok JL, Kopani KR, Amatruda JF, Murphey RD *et al*. (2005). *Curr Biol* **15**: 249–254.
Roy S, McPherson RA, Apolloni A, Yan J, Lane A, Clyde-Smith J *et al*. (1998). *Mol Cell Biol* **18**: 3947–3955.
Solit DB, Garraway LA, Pratilas CA, Sawai A, Getz G, Basso A *et al*. (2006). *Nature* **439**: 358–362.
Tanami H, Imoto I, Hirasawa A, Yuki Y, Sonoda I, Inoue J *et al*. (2004). *Oncogene* **23**: 8796–8804.
Terai K, Matsuda M. (2005). *EMBO Rep* **6**: 251–255.
Thiery JP. (2002). *Nat Rev Cancer* **2**: 442–454.
Tran NH, Frost JA. (2003). *J Biol Chem* **278**: 11221–11226.
Tran NH, Wu X, Frost JA. (2005). *J Biol Chem* **280**: 16244–16253.
Tsavachidou D, Coleman ML, Athanasiadis G, Li S, Licht JD, Olson MF *et al*. (2004). *Cancer Res* **64**: 5556–5559.
Wan PT, Garnett MJ, Roe SM, Lee S, Niculescu-Duvaz D, Good VM *et al*. (2004). *Cell* **116**: 855–867.
Wellbrock C, Karasarides M, Marais R. (2004a). *Nat Rev Mol Cell Biol* **5**: 875–885.
Wellbrock C, Ogilvie L, Hedley D, Karasarides M, Martin J, Niculescu-Duvaz D *et al*. (2004b). *Cancer Res* **64**: 2338–2342.
Wilhelm SM, Carter C, Tang L, Wilkie D, McNabola A, Rong H *et al*. (2004). *Cancer Res* **64**: 7099–7109.
Xiang X, Zang M, Waelde CA, Wen R, Luo Z. (2002). *J Biol Chem* **277**: 44996–45003.
Yaffe MB. (2002). *FEBS Lett* **513**: 53–57.
Yamaguchi T, Wallace DP, Magenheimer BS, Hempson SJ, Grantham JJ, Calvet JP. (2004). *J Biol Chem* **279**: 40419–40430.
Zhang BH, Guan KL. (2000). *EMBO J* **19**: 5429–5439.
Zhang BH, Tang ED, Zhu T, Greenberg ME, Vojtek AB, Guan KL. (2001). *J Biol Chem* **276**: 31620–31626.
Zhu J, Balan V, Bronisz A, Balan K, Sun H, Leicht DT *et al*. (2005). *Mol Biol Cell* **16**: 4733–4744.
Ziogas A, Moelling K, Radziwill G. (2005). *J Biol Chem* **280**: 24205–24211.